



## Secondary PM<sub>2.5</sub> in Zhengzhou, China: Chemical Species Based on Three Years of Observations

Jia Wang, Xiao Li, Wenkai Zhang, Nan Jiang, Ruiqin Zhang\*, Xiaoyan Tang

Research Institute of Environmental Science, College of Chemistry and Molecular Engineering, Zhengzhou University, Zhengzhou 450001, China

### ABSTRACT

The chemical properties and secondary components of PM<sub>2.5</sub> were investigated in the city of Zhengzhou, China. Water-soluble ionic species (Na<sup>+</sup>, NH<sub>4</sub><sup>+</sup>, K<sup>+</sup>, Mg<sup>2+</sup>, Ca<sup>2+</sup>, F<sup>-</sup>, Cl<sup>-</sup>, NO<sub>3</sub><sup>-</sup> and SO<sub>4</sub><sup>2-</sup>) contents, carbonaceous components (organic carbon (OC) and elemental carbon (EC)) in PM<sub>2.5</sub> were measured for three years. The EC tracer method was used to estimate the secondary organic carbon (SOC) content, and the Interagency Monitoring of Protected Visual Environments formula was used to estimate light extinction due to the chemical composition of PM<sub>2.5</sub>.

The annual mean concentrations of PM<sub>2.5</sub> were 186, 180 and 218 μg m<sup>-3</sup> in 2011, 2012 and 2013, respectively. These concentrations were 5–6 times greater than the National Ambient Air Quality Standards of China (annual value of 35 μg m<sup>-3</sup>) and indicated the presence of severe PM<sub>2.5</sub> pollution in Zhengzhou. Particulate organic matter (OM) contributed the most (18–26%) to the annual average PM<sub>2.5</sub>, followed by SO<sub>4</sub><sup>2-</sup> (14–19%), NO<sub>3</sub><sup>-</sup> (10–11%), NH<sub>4</sub><sup>+</sup> (8–9%) and EC (3%). From 2011 to 2013, the contributions of OM and SO<sub>4</sub><sup>2-</sup> increased by 8% and 3%, respectively. The higher sulfur oxidation ratio indicated the formation of significant amounts of secondary inorganic aerosols (SIA), particularly during the summer and spring. Obvious SOC enrichment occurred during the winter and autumn. In addition, SIA and secondary organic aerosols accounted for 26–50% and 4–21% of the PM<sub>2.5</sub> by mass, respectively. An investigation of the secondary species revealed that secondary aerosols played a dominant role in the total PM<sub>2.5</sub> mass and the decrease in visibility. The secondary aerosols ((NH<sub>4</sub>)<sub>2</sub>SO<sub>4</sub> + NH<sub>4</sub>NO<sub>3</sub> + SOC) accounted for 80% of *b*<sub>ext</sub>. The main secondary aerosols that led to poor visibility in Zhengzhou were (NH<sub>4</sub>)<sub>2</sub>SO<sub>4</sub> and NH<sub>4</sub>NO<sub>3</sub>.

**Keywords:** PM<sub>2.5</sub>; Water-soluble ionic species; Carbonaceous components; Secondary aerosols; Light extinction coefficient.

### INTRODUCTION

Since 2011, the frequency of haze in urban areas throughout the country has increased. Consequently, haze has become a serious problem in China, with persistent haze pollution events in China occurring in 2013. Action plans for controlling particulate pollution and decreasing PM<sub>2.5</sub> (atmospheric particulate matter with an aerodynamic diameter of less than 2.5 μm) emission limits have been developed by the Chinese State Council (CSC, 2013). However, due to rapid industrialization and urbanization, China's current coal-dominated energy structure has not changed (Wang *et al.*, 2006; Zhao, 2014). Moreover, the number of vehicles in China continues to increase, which is increasing the amount of fine particulate matter in the atmosphere and decreasing atmospheric visibility. Similar

to other megacities, Zhengzhou, which is the capital of Henan Province in central China, experiences serious particulate pollution problems and poor visibility (DEPH, 2013; EMSC, 2013). The primary pollutant in Zhengzhou during the daytime is PM<sub>2.5</sub>, which is responsible for 77% of polluted days (DEPH, 2014). Thus, haze occurs frequently in Zhengzhou.

PM<sub>2.5</sub> adversely affects human health (Valavanidis *et al.*, 2008; Anderson *et al.*, 2012) and visibility (Xu *et al.*, 2013). Furthermore, PM<sub>2.5</sub> contributes to global climate change by scattering light and increasing the amount of particles that can act as nuclei for cloud condensation (Chung and Seinfeld, 2002). PM<sub>2.5</sub> is a multi-component system that originates from both natural and anthropogenic sources (Alves *et al.*, 2000), and mainly consists of primary aerosols that are directly emitted from sources and secondary aerosols that are formed in the atmosphere. Secondary aerosols are mainly generated through a series of chemical reactions and physical processes that involve nitrogen oxides (NO<sub>x</sub>), sulfur dioxide (SO<sub>2</sub>), ammonia (NH<sub>3</sub>) and several volatile organic compounds (VOCs) that may react with ozone (O<sub>3</sub>), hydroxyl radicals (·OH) and other reactive

\* Corresponding author.

Tel.: 1-370-371-7002; Fax: 0371-67781163  
E-mail address: rqzhang@zzu.edu.cn

molecules to form sulfate ( $\text{SO}_4^{2-}$ ), nitrate ( $\text{NO}_3^-$ ), ammonium ( $\text{NH}_4^+$ ), secondary inorganic aerosols (SIA) and secondary organic carbon (SOC) (Liousse *et al.*, 1996; Squizzato *et al.*, 2013).

Aerosol measurements (Tao *et al.*, 2009; Deng *et al.*, 2013) have revealed that secondary chemical species strongly contribute to the overall concentration of fine particles in the atmosphere (approximately 50%). Therefore, secondary fractions are important for controlling  $\text{PM}_{2.5}$  pollution. Previous studies (Cabada *et al.*, 2002; Tao *et al.*, 2009; Behera and Sharma, 2010) have shown that secondary organic aerosols (SOA) are an important component of  $\text{PM}_{2.5}$ . The contributions of SOA to the total organic carbon (OC) concentration vary from nearly zero during the winter to 50% during the summer in Pittsburgh, Pennsylvania. In addition, SOC accounts for 29% of the OC concentration in  $\text{PM}_{2.5}$  in Guangzhou, China, and the SOA contents of  $\text{PM}_{2.5}$  during the winter and summer in Kanpur, India, are 18% and 12%, respectively. These aerosol species (SIA and SOA) are a significant cause of visibility degradation (Kim *et al.*, 2006; Tao *et al.*, 2009; Deng *et al.*, 2013) and vary between different seasons and regions. In addition, the Interagency Monitoring of Protected Visual Environments (IMPROVE) formula has been used to estimate the contributions of the chemical compositions of  $\text{PM}_{2.5}$  to light extinction, which helped determine the main factors of poor visibility (US EPA, 1999; Kim *et al.*, 2006; Hand *et al.*, 2011).

To better understand the secondary aerosol pollution conditions of  $\text{PM}_{2.5}$ , which have not been studied in Zhengzhou, the contributions of secondary species to the overall mass of  $\text{PM}_{2.5}$  and their impacts on visibility were investigated. The  $\text{PM}_{2.5}$  pollution levels and chemical properties (in terms of water-soluble ionic species and carbonaceous components) were determined in this study based on three years of measurements. Although many earlier studies have used short-term data, long-term data can more accurately reflect local pollution characteristics. In addition, the air quality trends shown in this study are helpful for understanding the effectiveness of pollution control strategies. Furthermore, this analysis will provide useful information for regulatory agencies and for creating strategies to control  $\text{PM}_{2.5}$  in the atmosphere.

## MATERIALS AND METHODS

### *Sampling and Mass Measurement*

Zhengzhou, the capital of Henan Province, is located in central China and has a temperate continental monsoon climate. In Zhengzhou, the average temperature is approximately 14.4°C, and the average annual precipitation is approximately 640 mm. Approximately 70% of the annual precipitation in Zhengzhou occurs from June to September. Southerly winds prevail during the summer, and northerly winds prevail during the winter. Due to rapid economic development, Zhengzhou has expanded to an area of 373 square kilometers and has a total population of over 4 million (an annual natural growth of approximately 59 thousand people).

$\text{PM}_{2.5}$  sample collections were conducted using quartz

microfiber filters (20.3 × 25.4 cm, PALL, USA) and a high-volume sampler (TE-6070D, Tisch Environmental, USA) from April 2011 to December 2013 at Zhengzhou University (Fig. 1). A TE-6070D sampler, which was equipped with a single-stage high-volume cascade impactor (TE-231, Tisch Environmental, USA), was used to remove particles larger than 10 μm. At least 15 samples were collected each season (winter, spring, summer and autumn) using a sampling duration of 22 h (9:00 AM–7:00 AM). The mass concentration of  $\text{PM}_{2.5}$  was determined using the gravimetric method. The filters were conditioned at  $20 \pm 5^\circ\text{C}$  before and after sampling at a relative humidity of  $50 \pm 5\%$  for at least 48 h before weighing on a microbalance (Mettler Toledo XS205, Switzerland) with a precision of 0.01 mg. Next, the samples were stored in a freezer ( $-18^\circ\text{C}$ ) until analysis.

### *Analysis of Water-Soluble Ions*

Ion concentrations ( $\text{Na}^+$ ,  $\text{NH}_4^+$ ,  $\text{K}^+$ ,  $\text{Mg}^{2+}$ ,  $\text{Ca}^{2+}$ ,  $\text{F}^-$ ,  $\text{Cl}^-$ ,  $\text{NO}_3^-$  and  $\text{SO}_4^{2-}$ ) were determined using an ion chromatograph (ICS-90, Dionex, USA). A circular punch with a known cross-sectional area was used to randomly intercept 2–6 pieces of the filter (including the middle and edge) in the sample zone. Furthermore, deionized water or an organic solvent was used to clean the punch before use. Two pieces of the samples were subjected to extractions using 25 mL of ultra-pure Milli-Q water (specific resistance: 18.2 MΩ cm). The samples were ultrasonicated in a water bath at  $< 30^\circ\text{C}$  for 30 min before filtering through 0.22 μm filters (Menbrana, German). The eluent used for detecting anions was composed of 8.0 mM  $\text{Na}_2\text{CO}_3$  and 1.0 mM  $\text{NaHCO}_3$ , and a flow rate of 0.8 mL  $\text{min}^{-1}$  was used. The eluent used for detecting cations was 20 mM methane sulfonic acid ( $\text{CH}_3\text{SO}_3\text{H}$ ), and a flow rate of 1.0 mL  $\text{min}^{-1}$  was used. All ions were identified based on their respective retention times.

### *Analysis of Carbon Species*

A piece of filter was removed from the 20.3 × 25.4 cm quartz filter and used for OC and elemental carbon (EC) analyses, which were conducted using an OC/EC analyzer (Sunset Laboratory, USA) and the thermal/optical transmission (TOT) method (Chow *et al.*, 2001). The detection limit was 0.2 μg  $\text{m}^{-3}$ , which was calculated as three times the standard deviation (SD) of the seven blank replicates. All analyses were conducted according to the NIOSH TOT protocol (low temperature in a helium atmosphere and high temperature in a 2% oxygen/98% helium atmosphere). A He–Ne laser (633 nm) was used to monitor sample transmission and correct for EC during OC pyrolysis at high temperatures.

### *Quality Assurance (QA) and Quality Control (QC)*

Field blank filters were analyzed to measure blank concentrations as part of QA/QC. The overall blank concentrations from the field blank samples were 0.02, 0.03, 0.00, 0.00, 0.03, 0.00, 0.01, 0.00 and 0.00 μg  $\text{m}^{-3}$  for  $\text{Na}^+$ ,  $\text{NH}_4^+$ ,  $\text{K}^+$ ,  $\text{Mg}^{2+}$ ,  $\text{Ca}^{2+}$ ,  $\text{F}^-$ ,  $\text{Cl}^-$ ,  $\text{NO}_3^-$  and  $\text{SO}_4^{2-}$ , respectively. In addition, the measured blank concentrations of EC and OC were 0.0 and 0.5 μg  $\text{m}^{-3}$ , respectively.

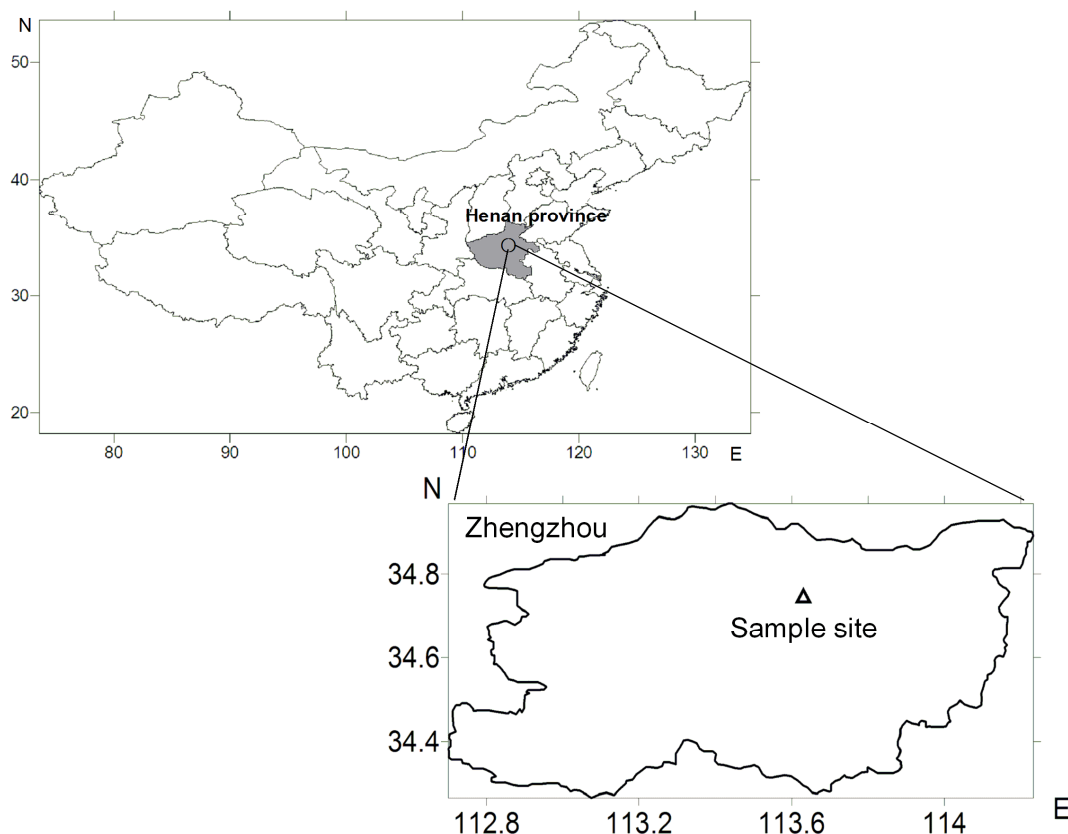


**Fig. 1.** Map of the sampling sites in Zhengzhou, Henan province, China.

The method detection limits (MDLs) of the ions were calculated as three times the noise and were 0.004, 0.017, 0.007, 0.006, 0.007, 0.009, 0.01, 0.07 and 0.05  $\mu\text{g m}^{-3}$  for  $\text{Na}^+$ ,  $\text{NH}_4^+$ ,  $\text{K}^+$ ,  $\text{Mg}^{2+}$ ,  $\text{Ca}^{2+}$ ,  $\text{F}^-$ ,  $\text{Cl}^-$ ,  $\text{NO}_3^-$  and  $\text{SO}_4^{2-}$ , respectively.

Ion recoveries in spiked calibration standard samples were determined to be 90–98%, 95–105%, 91–99%, 80–91%, 87–95%, 88–95%, 89–108%, 98–102% and 93–100% for  $\text{Na}^+$ ,  $\text{NH}_4^+$ ,  $\text{K}^+$ ,  $\text{Mg}^{2+}$ ,  $\text{Ca}^{2+}$ ,  $\text{F}^-$ ,  $\text{Cl}^-$ ,  $\text{NO}_3^-$  and  $\text{SO}_4^{2-}$ , respectively. Throughout sample testing, calibration standard curves were constructed that covered 4 orders of magnitude (0.5–100 ppm). Coefficients of  $> 0.999$  were obtained for the ions included in the study.

## RESULTS AND DISCUSSION

### *PM<sub>2.5</sub> Mass Concentration*

Overall, 66, 52 and 55  $\text{PM}_{2.5}$  samples were collected during 2011, 2012 and 2013, respectively, from the sampling site at Zhengzhou University, China. The  $\text{PM}_{2.5}$  concentrations ranged from 60 to 548  $\mu\text{g m}^{-3}$ , 55 to 565  $\mu\text{g m}^{-3}$  and 56 to 698  $\mu\text{g m}^{-3}$  in 2011, 2012 and 2013, respectively, with annual mean concentrations of 186, 180 and 218  $\mu\text{g m}^{-3}$ . Compared with the National Ambient Air Quality Standards of the USA (annual value of 15  $\mu\text{g m}^{-3}$ ) and the air quality guidelines of the World Health Organization (annual value of 10  $\mu\text{g m}^{-3}$ ), our results clearly indicated severe  $\text{PM}_{2.5}$  pollutions. In addition, the 3-year results (Fig. 2) showed that at least 90% of the daily  $\text{PM}_{2.5}$  concentrations exceeded

the proposed standards in China (75  $\mu\text{g m}^{-3}$  daily) that will be implemented on January 1, 2016.

The  $\text{PM}_{2.5}$  compositions and concentrations are presented in Table 1. The annual averages of  $\text{PM}_{2.5}$  and its components have steadily increased over time.  $\text{PM}_{2.5}$  results from primary anthropogenic emissions and the secondary transformation of gas pollutants in the atmosphere. Direct emissions mainly result from combustion of fossil fuels (coal, gasoline and diesel), biomass (straw and wood), and waste. The main gas pollutants that are converted into  $\text{PM}_{2.5}$  include  $\text{SO}_2$ ,  $\text{NO}_x$ ,  $\text{NH}_3$  and VOCs. Other anthropogenic sources include road dust, construction dust, industrial dust, kitchen smoke, etc. Zhengzhou is currently undergoing rapid economic development and urbanization. According to the Henan Statistical Yearbook of 2011–2013, the total energy consumption, number of vehicles, and population of Zhengzhou from 2011 to 2013 grew dramatically, with the greatest increase occurring in 2013 (Table 2). Increases in both  $\text{PM}_{2.5}$  and individual species are associated with increases in the number of vehicles and the total energy consumption in Zhengzhou. In addition, with the implementation of urban village reconstruction, construction dust has become a main source of  $\text{PM}_{2.5}$  emissions. Strong seasonal variations in  $\text{PM}_{2.5}$  were observed, with the highest concentrations occurring during the winter and the lowest concentrations occurring during the summer. The average  $\text{PM}_{2.5}$  concentrations during the winters of 2011, 2012 and 2013 were  $297 \pm 160$ ,  $234 \pm 12$  and  $337 \pm 168$   $\mu\text{g m}^{-3}$ , respectively, with corresponding summer values of  $120 \pm 40$ ,

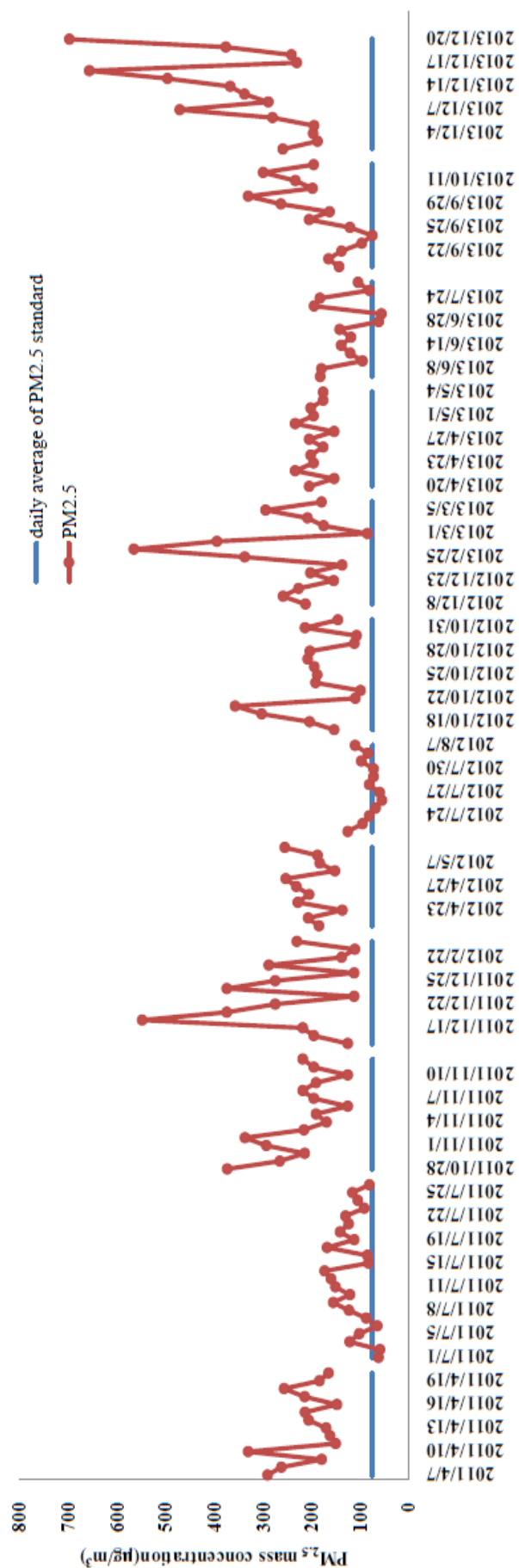


Fig. 2. Variations of daily  $PM_{2.5}$  concentrations from 2011 to 2013.

Table 1. Mean concentrations (mean  $\pm$  standard deviation (SD),  $\mu\text{g m}^{-3}$ ) of  $PM_{2.5}$  and the individual chemical species

	$PM_{2.5}$	$Na^+$	$NH_4^+$	$K^+$	$Mg^{2+}$	$Ca^{2+}$	$F^-$	$Cl^-$	$NO_3^-$	$SO_4^{2-}$	OC	EC
Spring	209 $\pm$ 56	1.7 $\pm$ 0.8	10 $\pm$ 5	2.3 $\pm$ 0.8	0.6 $\pm$ 0.2	5.5 $\pm$ 1.8	1.0 $\pm$ 0.5	5.1 $\pm$ 2.5	19 $\pm$ 10	26 $\pm$ 14	20 $\pm$ 4	5 $\pm$ 1
	202 (n = 11)	1.2 $\pm$ 0.2	19 $\pm$ 10	1.8 $\pm$ 1.1	0.5 $\pm$ 0.1	3.1 $\pm$ 0.9	0.4 $\pm$ 0.3	2.5 $\pm$ 1.3	14 $\pm$ 7	31 $\pm$ 16	17 $\pm$ 4	7 $\pm$ 2
	203 (n = 13)	1.1 $\pm$ 0.3	17 $\pm$ 6	2.1 $\pm$ 0.7	0.6 $\pm$ 0.2	6.8 $\pm$ 3.6	0.6 $\pm$ 0.4	2.0 $\pm$ 0.9	32 $\pm$ 13	58 $\pm$ 46	18 $\pm$ 3	6 $\pm$ 1
Summer	120 $\pm$ 40	0.4 $\pm$ 0.1	12 $\pm$ 7	0.8 $\pm$ 0.4	0.1 $\pm$ 0.1	0.8 $\pm$ 0.6	0.1 $\pm$ 0.1	1.1 $\pm$ 0.6	12 $\pm$ 7	31 $\pm$ 16	9 $\pm$ 4	5 $\pm$ 1
	2012 (n = 12)	0.3 $\pm$ 0.1	11 $\pm$ 5	0.6 $\pm$ 0.2	0.2 $\pm$ 0.1	1.7 $\pm$ 2.3	0.0 $\pm$ 0.0	0.4 $\pm$ 0.5	6 $\pm$ 6	24 $\pm$ 10	6 $\pm$ 2	4 $\pm$ 1
	2013 (n = 17)	0.5 $\pm$ 0.2	14 $\pm$ 10	1.3 $\pm$ 0.8	0.2 $\pm$ 0.1	2.4 $\pm$ 0.9	0.2 $\pm$ 0.3	1.2 $\pm$ 1.0	12 $\pm$ 12	33 $\pm$ 21	15 $\pm$ 9	5 $\pm$ 2
Autumn	222 $\pm$ 70	0.7 $\pm$ 0.4	13 $\pm$ 7	2.4 $\pm$ 1.0	0.2 $\pm$ 0.1	1.7 $\pm$ 1.1	0.6 $\pm$ 0.6	6.7 $\pm$ 3.7	24 $\pm$ 12	24 $\pm$ 11	31 $\pm$ 9	7 $\pm$ 3
	2012 (n = 15)	0.9 $\pm$ 0.4	14 $\pm$ 6	3.0 $\pm$ 0.8	0.3 $\pm$ 0.1	2.3 $\pm$ 1.2	0.8 $\pm$ 0.5	5.0 $\pm$ 2.3	26 $\pm$ 13	24 $\pm$ 8	34 $\pm$ 16	7 $\pm$ 3
	2013 (n = 14)	0.7 $\pm$ 0.3	15 $\pm$ 8	2.5 $\pm$ 1.0	0.3 $\pm$ 0.1	2.7 $\pm$ 1.8	0.3 $\pm$ 0.2	3.2 $\pm$ 2.5	21 $\pm$ 18	27 $\pm$ 22	31 $\pm$ 22	5 $\pm$ 3
Winter	297 $\pm$ 160	1.4 $\pm$ 1.1	21 $\pm$ 16	4.6 $\pm$ 2.8	0.2 $\pm$ 0.1	1.8 $\pm$ 0.7	1.0 $\pm$ 0.6	13.5 $\pm$ 7.4	31 $\pm$ 19	48 $\pm$ 36	45 $\pm$ 22	11 $\pm$ 5
	2012 (n = 14)	1.0 $\pm$ 0.6	16 $\pm$ 5	3.1 $\pm$ 1.3	0.3 $\pm$ 0.1	2.0 $\pm$ 1.5	0.8 $\pm$ 0.5	9.2 $\pm$ 4.7	22 $\pm$ 9	23 $\pm$ 10	35 $\pm$ 16	7 $\pm$ 4
	2013 (n = 15)	1.6 $\pm$ 0.6	31 $\pm$ 18	4.5 $\pm$ 1.9	0.5 $\pm$ 0.2	4.7 $\pm$ 1.9	1.5 $\pm$ 0.8	17.5 $\pm$ 10.3	39 $\pm$ 20	56 $\pm$ 39	54 $\pm$ 28	8 $\pm$ 3
Annual	186 $\pm$ 100	0.9 $\pm$ 0.9	15 $\pm$ 10	2.1 $\pm$ 2.0	0.3 $\pm$ 0.2	2.1 $\pm$ 2.1	0.5 $\pm$ 0.6	5.0 $\pm$ 5.9	20 $\pm$ 14	33 $\pm$ 22	22 $\pm$ 19	6 $\pm$ 4
	2012 (n = 52)	0.8 $\pm$ 0.5	15 $\pm$ 7	2.2 $\pm$ 1.4	0.3 $\pm$ 0.1	2.3 $\pm$ 1.6	0.5 $\pm$ 0.5	4.6 $\pm$ 4.4	18 $\pm$ 12	25 $\pm$ 11	24 $\pm$ 17	6 $\pm$ 3
	2013 (n = 55)	1.0 $\pm$ 0.6	19 $\pm$ 14	2.7 $\pm$ 1.8	0.4 $\pm$ 0.2	4.1 $\pm$ 2.8	0.7 $\pm$ 0.7	6.6 $\pm$ 9.0	27 $\pm$ 19	44 $\pm$ 32	33 $\pm$ 25	6 $\pm$ 3

**Table 2.** Civil vehicles, total energy consumption and population of Zhengzhou from 2011 to 2013.

Year	Civil vehicles in millions of cars	Total energy consumption in millions of tons of standard coal equivalent	Population in millions
2011	1.24	30.10	8.86
2012	1.43	31.81	9.03
2013	1.72	35.97	9.19

Notes: Henan Statistical Yearbook 2012–2014.

$84 \pm 21$  and  $128 \pm 47 \mu\text{g m}^{-3}$ . Each species (except  $\text{SO}_4^{2-}$ ) exhibited consistent  $\text{PM}_{2.5}$  trends, with the highest  $\text{PM}_{2.5}$  levels occurring during the winter and the lowest levels occurring during the summer. The  $\text{SO}_4^{2-}$  concentrations in  $\text{PM}_{2.5}$  were lowest in the autumn.

The seasonal  $\text{SO}_4^{2-}$  concentrations of  $\text{PM}_{2.5}$  ranged from  $23 \pm 10 \mu\text{g m}^{-3}$  (winter of 2012) to  $58 \pm 46 \mu\text{g m}^{-3}$  (spring of 2013). Regarding the seasonal average, the magnitudes of  $\text{SO}_4^{2-}$  in the  $\text{PM}_{2.5}$  decreased as follows: winter ( $23\text{--}56 \mu\text{g m}^{-3}$ ) > spring ( $26\text{--}58 \mu\text{g m}^{-3}$ ) > summer ( $24\text{--}35 \mu\text{g m}^{-3}$ ) > autumn ( $24\text{--}27 \mu\text{g m}^{-3}$ ). The seasonal variations in the average  $\text{NO}_3^-$  concentrations decreased as follows: winter ( $22\text{--}39 \mu\text{g m}^{-3}$ ) > autumn ( $21\text{--}26 \mu\text{g m}^{-3}$ ) > spring ( $14\text{--}32 \mu\text{g m}^{-3}$ ) > summer ( $6\text{--}13 \mu\text{g m}^{-3}$ ). In addition, the seasonal  $\text{NH}_4^+$  concentrations in  $\text{PM}_{2.5}$  decreased as follows: winter ( $16\text{--}31 \mu\text{g m}^{-3}$ ) > spring ( $10\text{--}19 \mu\text{g m}^{-3}$ )  $\approx$  autumn ( $13\text{--}15 \mu\text{g m}^{-3}$ )  $\approx$  summer ( $11\text{--}14 \mu\text{g m}^{-3}$ ). However, in contrast with  $\text{SO}_4^{2-}$ , the  $\text{NO}_3^-$  and  $\text{NH}_4^+$  concentrations in  $\text{PM}_{2.5}$  were lowest during the summer.

The results shown in Table 1 indicated that  $\text{SO}_4^{2-}$ , OC,  $\text{NO}_3^-$ ,  $\text{NH}_4^+$  and EC were the main species of the analyzed components in  $\text{PM}_{2.5}$ . The mass contributions of these chemical species to  $\text{PM}_{2.5}$  were calculated for the annual samples (Fig. 3). The particulate organic matter (OM) shown in Fig. 3 was obtained by multiplying OC by 1.6 (Turpin and Lim, 2001). The other ions, including  $\text{Na}^+$ ,  $\text{K}^+$ ,  $\text{Mg}^{2+}$  and  $\text{F}^-$ , were individual species with relatively low concentrations. The non-apportioned portion was obtained by subtracting the OM, EC and nine water-soluble ions from the total mass of  $\text{PM}_{2.5}$ .

As observed from the annual average (Fig. 3), OM contributed the most (18–26%) to  $\text{PM}_{2.5}$ , followed by  $\text{SO}_4^{2-}$  (14–19%),  $\text{NO}_3^-$  (10–11%),  $\text{NH}_4^+$  (8–9%) and EC (3%). From 2011 to 2013, the contributions of each of these species increased, except for the contribution of EC which did not change. Among these species, the contributions of OM increased by 8% and the contributions of  $\text{SO}_4^{2-}$  increased by 3%. The contributions of the non-apportioned species decreased from 40% (2011) to 25% (2013), which indicated that the proportions of OM,  $\text{SO}_4^{2-}$ ,  $\text{NO}_3^-$  and  $\text{NH}_4^+$  in  $\text{PM}_{2.5}$  increased.

Regarding the non-apportioned portion, the results of our study were comparable with those observed in a previous study conducted in Beijing, in which approximately 35%–48% of  $\text{PM}_{2.5}$  was non-apportioned (Hu *et al.*, 2015). Several scientific studies have shown that quartz filters, which show a higher retention of organics and lower release of ammonium salts (Schaap *et al.*, 2004; Wittmaack and Keck, 2004; Vecchi *et al.*, 2009), tend to absorb more water vapor due to their hydrophilic nature and wettability

(Zdziennicka *et al.*, 2009). This water vapor would contribute to the non-apportioned mass. In addition, Hu (Hu *et al.*, 2015) inferred that approximately 15%–32% of  $\text{PM}_{2.5}$  in the quartz filters was from water vapor.

In terms of the annual trends, the mass concentration of the non-apportioned part and its contribution to the total PM mass decreased each year. According to our previous study (Geng *et al.*, 2013), the contribution of dust to  $\text{PM}_{2.5}$  was 26%. If the non-apportioned portion represents only one source, we believe that it is most likely resuspended dust (including soil dust, construction dust and road dust). However, we did not measure metal concentrations in this study, which is an area that warrants future study.

Accordingly, we attribute the non-apportioned portions in this study to metal oxides, water and undefined chemical species (refractory or insoluble).

Fig. 4 shows the percentages of the chemical species in the seasonally sampled  $\text{PM}_{2.5}$ . Among the spring samples, the contributions of OM, EC,  $\text{NH}_4^+$ ,  $\text{Cl}^-$ ,  $\text{Ca}^{2+}$  and the other ions changed very little over the years studied (1%). Large increases in the  $\text{SO}_4^{2-}$  (15–30%),  $\text{NO}_3^-$  (9–16%), and  $\text{NH}_4^+$  (5–9%) occurred in 2013 relative to the 2011 and 2012 values.

The contribution of OM in the summer samples was 12% in 2011 and 2012 and increased by 7% in 2013. The contributions of  $\text{SO}_4^{2-}$ ,  $\text{NO}_3^-$  and  $\text{NH}_4^+$  varied from 25% (2013) to 29% (2012), 7% (2012) to 9% (2013) and 11% (2013) to 13% (2012), respectively. Meanwhile, the contributions of OM,  $\text{SO}_4^{2-}$  and  $\text{NH}_4^+$  in the autumn samples increased steadily by 8%, 6% and 2%, respectively, from 2011 to 2013. The contributions of OM,  $\text{SO}_4^{2-}$ ,  $\text{NO}_3^-$  and  $\text{NH}_4^+$  varied from 22% (2011) to 30% (2013), 10% (2011) to 16% (2013), 11% (2011) to 14% (2012) and 6% (2011) to 8% (2013), respectively. Based on the winter samples, the contributions of each constituent were the same for 2011 and 2013. The contributions of OM and  $\text{SO}_4^{2-}$  were lower in 2012 (OM: 24%,  $\text{SO}_4^{2-}$ : 10%) than in 2011 and 2013 (OM: 27%,  $\text{SO}_4^{2-}$ : 16%), and the contributions of  $\text{NO}_3^-$  and  $\text{NH}_4^+$  varied from 10% (2011) to 12% (2013) and 7% (2012) to 9% (2013), respectively.

Overall, OM comprised a larger percentage of the  $\text{PM}_{2.5}$  during the autumn and winter (22–30%). The maximum contributions of  $\text{Cl}^-$  to  $\text{PM}_{2.5}$  occurred during the winter and reached 5%. Coal combustion releases significant amounts of chlorine (McCulloch *et al.*, 1999); thus, fine particles are enriched in OC and  $\text{Cl}^-$  in areas that use coal-fire heat during the winter.

The maximum contributions of  $\text{SO}_4^{2-}$  (25–29%) and  $\text{NH}_4^+$  (11–13%) to  $\text{PM}_{2.5}$  occurred during the summer, while the maximum contribution of  $\text{NO}_3^-$  occurred during the autumn

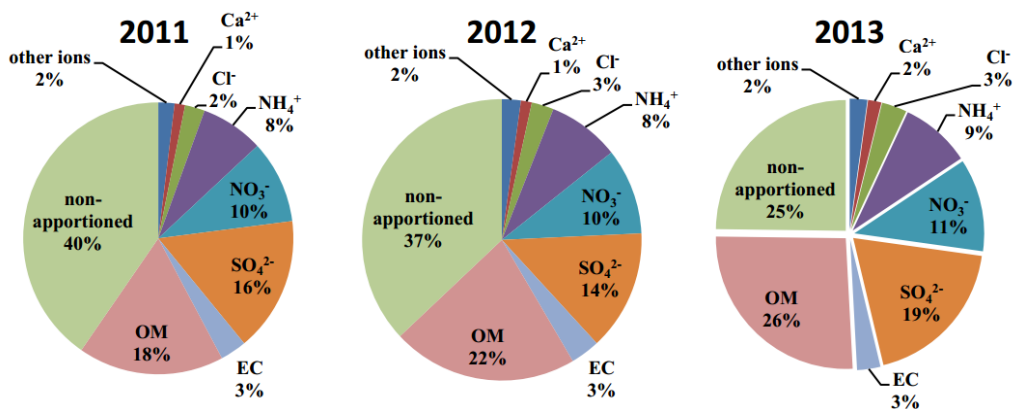


Fig. 3. Annual mean contributions of the individual components to PM<sub>2.5</sub>.

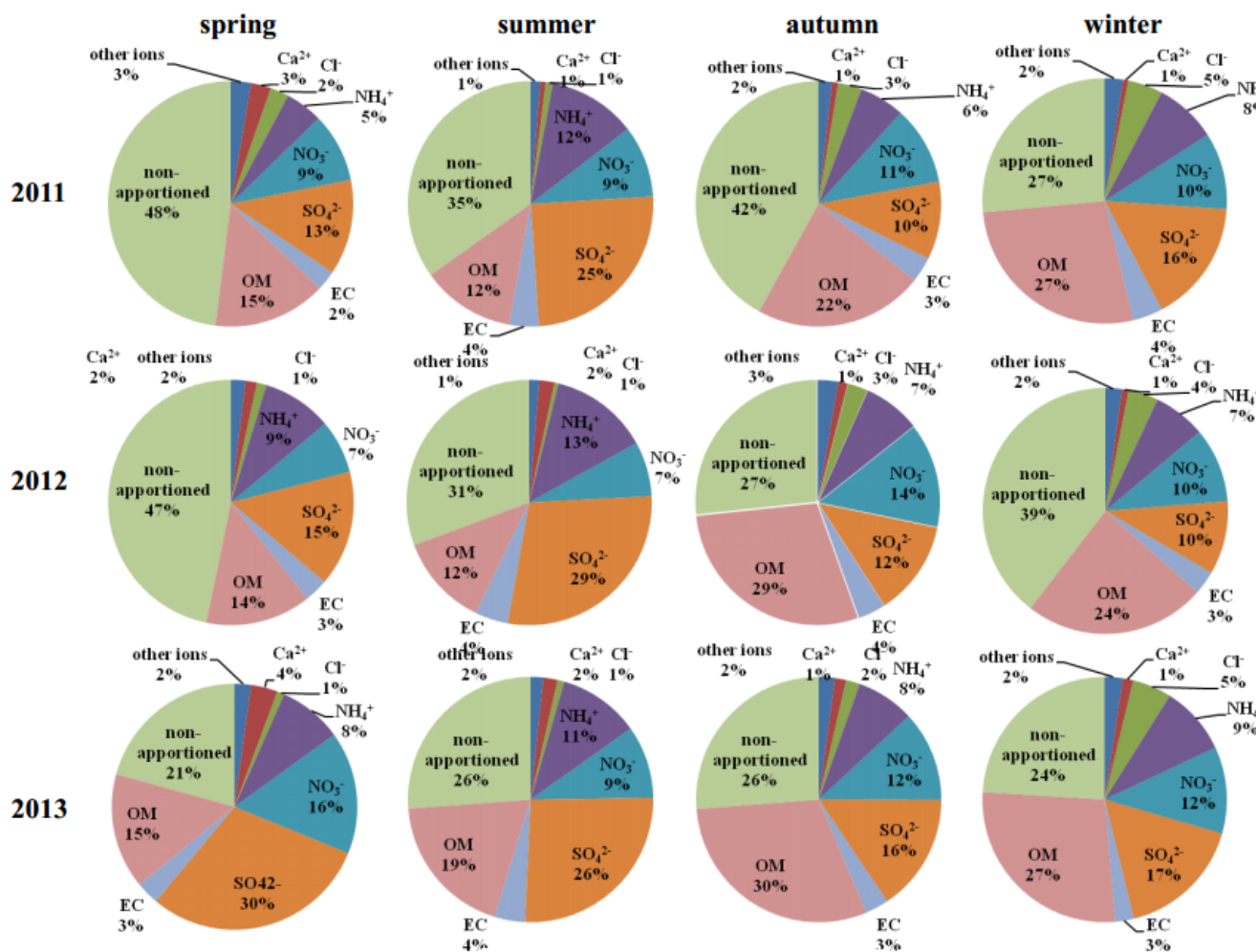


Fig. 4. Seasonal contributions of the individual components to PM<sub>2.5</sub>.

(11–14%) and differed from the contributions of SO<sub>4</sub><sup>2-</sup> and NH<sub>4</sub><sup>+</sup>. This observation may be attributed to the volatility of ammonium nitrate, which is the main chemical form of nitrate and can evaporate when subjected to the relatively high temperatures that occur during the summer (Wang *et al.*, 2005). The different seasonal trends observed in the three major secondary species resulted from the differences in their formation mechanisms and the seasonal variations of the

meteorological conditions in Zhengzhou. The contributions of Ca<sup>2+</sup> (the crustal ion) to the PM<sub>2.5</sub> were 2–4% greater during the spring than during the other seasons because sandstorms frequently occurred during the spring.

### Ionic Components and Carbonaceous Species

#### Ionic Components

To describe the magnitude of the transformation of

atmospheric SO<sub>2</sub> to SO<sub>4</sub><sup>2-</sup> and NO<sub>2</sub> to NO<sub>3</sub><sup>-</sup>, the sulfur oxidation ratio (SOR) and nitrogen oxidation ratio (NOR) were calculated (Wang *et al.*, 2005; Gao *et al.*, 2011). The SOR and NOR are defined as follows:

$$SOR = \frac{n - SO_4^{2-}}{n - SO_4^{2-} + n - SO_2} \quad (1)$$

$$NOR = \frac{n - NO_3^-}{n - NO_3^- + n - NO_2} \quad (2)$$

where  $n - SO_4^{2-}$ ,  $n - SO_2$ ,  $n - NO_3^-$  and  $n - NO_2$  are the molar concentrations of SO<sub>4</sub><sup>2-</sup>, SO<sub>2</sub>, NO<sub>3</sub><sup>-</sup> and NO<sub>2</sub>, respectively. The concentrations of SO<sub>2</sub> and NO<sub>2</sub> were obtained from air quality monitoring stations operated by the Environmental Protection Bureau of Zhengzhou, which is located four kilometers from the sampling site.

The seasonal average conversion ratios for sulfate and nitrate were calculated for PM<sub>2.5</sub> in Zhengzhou (Table 3). The sulfate conversion fractions were greater during the summer (0.4 ± 0.2) and spring (0.4 ± 0.1) and were relatively constant (0.2 ± 0.1) during the autumn and winter. The mean values of NOR were similar during all four seasons (0.2 ± 0.1). Previous studies have reported SOR values of < 0.10 in the flue gas of oil combustion boilers (Kircher *et al.*, 1977) and < 0.027 in vehicle exhaust (Pierson *et al.*, 1979; Truex *et al.*, 1980). Coal-fired boilers are commonly used in China. According to a study conducted by Wang (Wang *et al.*, 2008), the SOR in the flue gas of coal-fired power plants is much less than 0.10. Therefore, 0.10 is

regarded as a conservative (i.e., maximum) SOR value for primary pollutants. Thus, atmospheric SORs > 0.10 suggest the occurrence of photochemical oxidation of SO<sub>2</sub>.

As shown in Table 3, significant amounts of secondary SO<sub>4</sub><sup>2-</sup> were generated during all four seasons, and conditions that are more favorable for formation occurred during the summer and spring. In this study, the seasonal variations of SOR (or NOR) are not obvious.

The equivalent ratio of [NH<sub>4</sub><sup>+</sup>]/([NO<sub>3</sub><sup>-</sup>] + 2[SO<sub>4</sub><sup>2-</sup>]) in PM<sub>2.5</sub> (Squizzato *et al.*, 2013; Voutsas *et al.*, 2014) was calculated in Table 4. These values were >1.0, except during the spring, which indicated that excess NH<sub>4</sub> was present. The mass ratio of NO<sub>3</sub><sup>-</sup>/SO<sub>4</sub><sup>2-</sup> was used as an indicator of the relative importance of mobile vs. stationary sources in this study (Yao *et al.*, 2002; Wang *et al.*, 2006; Gao *et al.*, 2011). According to Yao *et al.* (2002), the estimated ratios of NO<sub>x</sub> to SO<sub>x</sub> in gasoline, diesel fuel and coal combustion emissions are 13:1, 8:1 and 1:2, respectively. In addition, high NO<sub>3</sub><sup>-</sup>/SO<sub>4</sub><sup>2-</sup> mass ratios result from a predominance of mobile sources over stationary sources. High NO<sub>3</sub><sup>-</sup>/SO<sub>4</sub><sup>2-</sup> mass ratios have been reported in southern California, with values of 2 in downtown Los Angeles and 5 in Rubidoux due to low coal use (Kim *et al.*, 2000). As shown in Table 4, the mean NO<sub>3</sub><sup>-</sup>/SO<sub>4</sub><sup>2-</sup> mass ratios for the seasonal samples in this study were approximately 0.3–1.1. Therefore, stationary source emissions were more important for contributing fine particles in the study area.

#### EC and OC

The seasonal EC and OC concentrations are summarized in Table 1. The OC concentrations were highest during the

**Table 3.** Calculated sulfur and nitrogen oxidation ratios (SOR and NOR) of PM<sub>2.5</sub>.

		Spring	Summer	Autumn	Winter
SOR	2011	0.4 ± 0.1	0.4 ± 0.2	0.3 ± 0.1	0.2 ± 0.1
	2012	0.5 ± 0.2	0.5 ± 0.1	0.2 ± 0.1	0.2 ± 0.1
	2013	0.3 ± 0.2	0.4 ± 0.2	0.2 ± 0.1	0.2 ± 0.2
	ave	0.4 ± 0.1	0.4 ± 0.2	0.2 ± 0.1	0.2 ± 0.1
NOR	2011	0.2 ± 0.1	0.2 ± 0.1	0.3 ± 0.1	0.3 ± 0.1
	2012	0.2 ± 0.1	0.2 ± 0.2	0.2 ± 0.1	0.2 ± 0.1
	2013	0.3 ± 0.1	0.2 ± 0.2	0.2 ± 0.1	0.2 ± 0.1
	ave	0.2 ± 0.1	0.2 ± 0.1	0.2 ± 0.1	0.2 ± 0.1

**Table 4.** Neutralization ratio (NR) and NO<sub>3</sub><sup>-</sup>/SO<sub>4</sub><sup>2-</sup> (mean ± SD).

		[NH <sub>4</sub> <sup>+</sup> ]/([NO <sub>3</sub> <sup>-</sup> ] + 2[SO <sub>4</sub> <sup>2-</sup> ])	NO <sub>3</sub> <sup>-</sup> /SO <sub>4</sub> <sup>2-</sup>
Spring	2011	0.7 ± 0.1	0.8 ± 0.2
	2012	1.2 ± 0.2	0.5 ± 0.1
	2013	0.6 ± 0.2	0.7 ± 0.4
Summer	2011	1.0 ± 0.1	0.4 ± 0.1
	2012	1.0 ± 0.2	0.3 ± 0.2
	2013	1.2 ± 1.6	0.3 ± 0.3
Autumn	2011	1.4 ± 2.0	1.1 ± 0.4
	2012	0.9 ± 0.1	1.1 ± 0.3
	2013	1.4 ± 2.2	0.7 ± 0.3
Winter	2011	1.0 ± 0.2	0.8 ± 0.4
	2012	1.1 ± 0.2	1.0 ± 0.4
	2013	1.0 ± 0.4	0.8 ± 0.2

winter (2011:  $45 \pm 22 \mu\text{g m}^{-3}$ ; 2012:  $35 \pm 16 \mu\text{g m}^{-3}$  and 2013:  $54 \pm 28 \mu\text{g m}^{-3}$ ), followed by autumn, spring and summer, probably due to the combined effects of enhanced emissions from coal combustion for residential heating and stable atmospheric conditions during the winter (Duarte *et al.*, 2008). The mean OC concentrations during the summer of 2013 ( $15 \pm 9 \mu\text{g m}^{-3}$ ) were much higher than those during the summer of 2011 ( $9 \pm 4 \mu\text{g m}^{-3}$ ) and 2012 ( $6 \pm 2 \mu\text{g m}^{-3}$ ). The EC concentrations showed no strong seasonal variations, except for slightly higher concentrations during the winter.

The annual mean concentrations of OC in  $\text{PM}_{2.5}$  were  $22 \pm 19$ ,  $24 \pm 17$  and  $33 \pm 25 \mu\text{g m}^{-3}$  in 2011, 2012 and 2013, respectively. The annual mean EC values were the same for all three years ( $6 \pm 3 \mu\text{g m}^{-3}$ ), as shown in Table 1. The combined effects of greater energy consumption and improved combustion technology resulted in higher OC levels and stable EC levels.

The OC/EC ratios are presented in Table 5. In this study, the OC/EC ratios were ordered as follows: autumn ( $5.3 \pm 1.8$ ) > winter ( $4.4 \pm 1.4$ ) > spring ( $3.7 \pm 0.8$ ) > summer ( $1.9 \pm 0.6$ ) in 2011; winter ( $5.2 \pm 2.4$ ) > autumn ( $4.9 \pm 0.9$ ) > spring ( $2.7 \pm 0.5$ ) > summer ( $1.8 \pm 0.5$ ) in 2012; and winter ( $7.0 \pm 3.1$ ) > autumn ( $5.7 \pm 3.3$ ) > summer ( $3.8 \pm 2.7$ ) > spring ( $3.3 \pm 0.7$ ) in 2013.

Each of the source materials resulted in a different OC/EC ratio when burned. The reported OC/EC ratios of typical emission sources are: 1.0–4.2 for diesel- and gasoline-powered vehicular exhaust (Schauer *et al.*, 1999, 2002); 2.5–10.5 for residential coal smoke (Chen *et al.*, 2006); and 7.7 for cereal straw burning (Zhang *et al.*, 2007). The OC/EC ratios reported by Koch *et al.* (2007) using the NASA Goddard Global Climate Model were < 1 for fossil fuel burning and > 5 for biomass burning.

In this study, the OC/EC ratios were 3.3 and 2.6 during the spring and summer, respectively, which were in the OC/EC ratio ranges of petrochemical fuel (< 1) and residential coal-fired emissions (2.5–10.5). The OC/EC ratios were 5.4 and 6 during the autumn and winter, respectively, which corresponded to the OC/EC ratios of coal (2.5–10.5) and biomass (> 5) burning. Therefore, we concluded that fossil fuels (petrol, gasoline and coal) may be dominant during the spring and summer and that coal smoke and biomass

burning were the main sources of OC and EC emissions during the autumn and winter.

In our previous study, the sources of  $\text{PM}_{2.5}$  in Zhengzhou included dust (26%), secondary aerosols (24%), coal combustion (23%), biomass burning/oil combustion/incineration (13%), vehicular emissions (10%) and industrial emissions (4%) (Geng *et al.*, 2013). In 2011, coal consumption in Zhengzhou accounted for 78% of the total energy consumption, and oil accounted for 9% (Zhou, 2013). No statistics were available regarding biomass energy. The results of this study are consistent with those of our study and indicate the presence of a coal-dominated energy structure in Zhengzhou. Biomass energy sources, such as straw and wood, are traditional non-commercial energy sources that are dominant in rural areas. These energy sources are particularly used in households for cooking and domestic heating during the winter through direct combustion. Straw is an important component of energy consumption.

### Secondary Aerosols

#### SOC

Directly quantifying primary and secondary organic components in  $\text{PM}_{2.5}$  using chemical analysis is difficult. Several studies have estimated SOC using an EC tracer method that considers the minimum ratio of OC/EC as a constant mixture of primary OC and EC (Castro *et al.*, 1999; Cabada *et al.*, 2002, 2004; Duarte *et al.*, 2008).

The SOC can be calculated using the following equation:

$$\text{SOC} = \text{OC} - \text{EC} \left( \frac{\text{OC}}{\text{EC}} \right)_{\min} \quad (3)$$

In this study, the minimum ratios of OC to EC were 1.69, 1.09, 1.86 and 2.29 for spring, summer, autumn and winter, respectively, which were similar to the ratios observed during the summer (1.08) and winter (2.32) by Cao *et al.* (2007). The estimated SOC concentrations are presented in Table 5. The SOC fraction in  $\text{PM}_{2.5}$  varied as follows: winter ( $20 \pm 13 \mu\text{g m}^{-3}$ ) > autumn ( $16 \pm 9 \mu\text{g m}^{-3}$ ) > spring ( $10 \pm 3 \mu\text{g m}^{-3}$ ) > summer ( $4 \pm 3 \mu\text{g m}^{-3}$ ) in 2011; autumn ( $21 \pm 12 \mu\text{g m}^{-3}$ ) > winter ( $19 \pm 13 \mu\text{g m}^{-3}$ ) > spring

**Table 5.** Seasonal OC/EC ratios, SOC and SIA fraction contributions to  $\text{PM}_{2.5}$

		OC/EC	SOC $\mu\text{g m}^{-3}$	SOC/OC %	SIA $\mu\text{g m}^{-3}$	SPM $\mu\text{g m}^{-3}$
Spring	2011	$3.7 \pm 0.8$	$10 \pm 3$	$53 \pm 8$	$56 \pm 27$	$66 \pm 27$
	2012	$2.7 \pm 0.5$	$7 \pm 2$	$39 \pm 9$	$64 \pm 32$	$71 \pm 32$
	2013	$3.2 \pm 0.5$	$8 \pm 3$	$47 \pm 8$	$98 \pm 47$	$107 \pm 48$
Summer	2011	$1.9 \pm 0.6$	$4 \pm 3$	$39 \pm 19$	$52 \pm 24$	$56 \pm 25$
	2012	$1.8 \pm 0.5$	$2 \pm 2$	$35 \pm 19$	$41 \pm 16$	$43 \pm 16$
	2013	$3.8 \pm 2.7$	$10 \pm 7$	$56 \pm 19$	$49 \pm 40$	$74 \pm 42$
Autumn	2011	$5.3 \pm 1.8$	$16 \pm 9$	$56 \pm 22$	$59 \pm 24$	$76 \pm 27$
	2012	$4.9 \pm 0.9$	$21 \pm 12$	$60 \pm 8$	$64 \pm 26$	$84 \pm 35$
	2013	$5.7 \pm 3.3$	$25 \pm 19$	$62 \pm 17$	$63 \pm 43$	$90 \pm 53$
Winter	2011	$4.4 \pm 1.4$	$20 \pm 13$	$44 \pm 16$	$91 \pm 55$	$111 \pm 66$
	2012	$5.2 \pm 2.4$	$19 \pm 13$	$49 \pm 22$	$61 \pm 21$	$83 \pm 27$
	2013	$7.0 \pm 3.1$	$39 \pm 24$	$63 \pm 14$	$125 \pm 76$	$164 \pm 98$

( $7 \pm 2 \mu\text{g m}^{-3}$ ) > summer ( $2 \pm 2 \mu\text{g m}^{-3}$ ) in 2012; and winter ( $39 \pm 24 \mu\text{g m}^{-3}$ ) > autumn ( $25 \pm 19 \mu\text{g m}^{-3}$ ) > summer ( $10 \pm 7 \mu\text{g m}^{-3}$ ) > spring ( $8 \pm 3 \mu\text{g m}^{-3}$ ) in 2013.

In 2011 and 2012, the maximum SOC to OC ratios occurred during the autumn ( $56 \pm 22\%$  and  $60 \pm 8\%$ , respectively), and the minimum ratios ( $39 \pm 19\%$  and  $35 \pm 19\%$ , respectively) occurred during the summer. In 2013, the lowest SOC to OC ratio occurred during the spring ( $47 \pm 8\%$ ) and increased to > 62% during the autumn and winter. This result clearly indicated that the OC was dominated by SOC. On average, the contributions of SOC to  $\text{PM}_{2.5}$  were 3–5, 3–10, 6–12 and 8–11% during the spring, summer, autumn and winter, respectively. This seasonal pattern (i.e., the contribution being highest in winter) was consistent with the results for Xiamen, as reported by Niu *et al.* (2012); however, these results were different from those obtained by Castro *et al.* (1999) and Cao *et al.* (2007), who reported that minimum SOC production occurred during the winter. SOC was formed from the atmospheric oxidation of volatile organic compounds (VOCs) and subsequent gas-to-particle conversion processes. In the study by Niu *et al.* (2012), it was concluded that low humidity, suitable temperatures (4–20°C) and low sunlight were advantageous for the formation of SOC. Temperature had a dramatic effect on the formation of secondary organic aerosols; the formation of SOA was approximately 2.5–6 times greater at 5°C (the lowest temperature studied) than at > 27°C (Warren *et al.*, 2009). The climate of Zhengzhou is dry, with an annual average temperature of 14°C (–1 to 9°C in winter) and moderate sunlight, which may be favorable for the formation of SOC.

Meanwhile, greater emissions from residential heating (from mid-November to mid-March) could significantly contribute to the formation of the SOC fraction. The largest anthropogenic source of VOCs in Henan was stationary combustion (mainly residential coal combustion and biomass burning) (Fan *et al.*, 2012). Zhengzhou is the provincial capital of Henan province and is surrounded by several rural areas. Biomass energy sources, such as straw and wood, have long been used as traditional non-commercial energy sources and dominate the energy consumption in rural areas. As the rural economy improved and lifestyles changed, the proportion of non-commercial energy decreased, stabilizing at approximately 50% after 2000 (Shi *et al.*, 2010). However, straw consumption remained stable, and straw remains an important energy source.

Overall, the enrichment of SOC during autumn and winter is due to an increase in the emissions from residential coal and biomass combustion and the low-temperature transformation of VOCs and their condensation on particulate matter.

### Secondary Components

The SIA fraction and the secondary particulate matter (SPM) fraction are summarized in Table 5. The highest SIA occurred during the winter ( $125 \pm 76 \mu\text{g m}^{-3}$ ), and the lowest occurred during the summer ( $41 \pm 16 \mu\text{g m}^{-3}$ ). A similar seasonal pattern was observed for SPM, with concentrations of  $43 \pm 16 \mu\text{g m}^{-3}$  during the summer and  $164 \pm 98 \mu\text{g m}^{-3}$  during the winter.

To understand the secondary aerosol pollution conditions,

the contributions of secondary species to the overall  $\text{PM}_{2.5}$  mass are shown in Fig. 5. On average, the contributions of SIA ( $\text{NH}_4^+$ ,  $\text{SO}_4^{2-}$  and  $\text{NO}_3^-$ ) to  $\text{PM}_{2.5}$  decreased as follows: summer (41–50%) > winter (26–36%)  $\approx$  autumn (26–35%) > spring (27–33%). The contributions of SOA to  $\text{PM}_{2.5}$  were 5–8%, 4–19%, 18–21% and 13–17% during the spring, summer, autumn and winter, respectively. The results showed the same seasonal trends as reported by Behera and Sharma (2010) for Kanpur, India, who concluded that the SIA and SOA of  $\text{PM}_{2.5}$  were approximately 34% and 12% in the summer and 32% and 18% in the winter, respectively.

Regarding the annual average, SIA accounted for 35%, 33% and 38% of the  $\text{PM}_{2.5}$  during 2011, 2012 and 2013, respectively, with corresponding SOA contributions of 9%, 12% and 18%, respectively. Secondary aerosols accounted for 35–41%, 54–60%, 36–56% and 39–53% of the  $\text{PM}_{2.5}$  mass during the spring, summer, autumn and winter, respectively, with the greatest contributions occurring during the summer of 2013 and the lowest contributions occurring during the spring of 2011. Thus, secondary aerosols, which comprise a large fraction of  $\text{PM}_{2.5}$ , are important.

### Visibility Degradation Impacts

The light extinction coefficient ( $b_{\text{ext}}$ ) was estimated using the following formula proposed by the IMPROVE program and by applying the  $\text{PM}_{2.5}$  chemical composition measurements to reconstruct  $b_{\text{ext}}$  (IMPROVE, a):

$$b_{\text{ext}} = (3)f(\text{RH})[\text{SULFATE}] + (3)f(\text{RH})[\text{NITRATE}] + (4)[\text{OMC}] + (10)[\text{LAC}] + (1)[\text{SOIL}] + (0.6)[\text{CM}]$$

The definitions of the species are as follows: [SULFATE] is  $(\text{NH}_4)_2\text{SO}_4 = 1.37[\text{SO}_4^{2-}]$ ; [NITRATE] is  $\text{NH}_4\text{NO}_3 = 1.29[\text{NO}_3^-]$ ; [OMC] (organic mass by carbon) =  $1.4[\text{OC}]$ ; [LAC] (light absorbing carbon) = [EC]; [SOIL] (fine soil) =  $2.2[\text{Al}] + 2.49[\text{Si}] + 1.63[\text{Ca}] + 2.42[\text{Fe}] + 1.94[\text{Ti}]$ ; [CM] (coarse mass) =  $[\text{PM}_{10}] - [\text{PM}_{2.5}]$ .  $b_{\text{ext}}$  has units of  $\text{Mm}^{-1}$ . The brackets indicate the average mass concentrations of the aerosol species. The specific dry scattering efficiency is  $3 \text{ m}^2 \text{ g}^{-1}$  for ammonium sulfate and ammonium nitrate,  $4 \text{ m}^2 \text{ g}^{-1}$  for organic carbon,  $1 \text{ m}^2 \text{ g}^{-1}$  for soil, and  $0.6 \text{ m}^2 \text{ g}^{-1}$  for coarse mass. In addition, the specific absorption efficiency for LAC is  $10 \text{ m}^2 \text{ g}^{-1}$ . The relative humidity scattering enhancement factor,  $f(\text{RH})$ , was defined as 2 in this study based on the IMPROVE monitoring network (IMPROVE, b) and the annual average relative humidity of Zhengzhou (67%).

In our previous study, crust and trace elements only comprised 2–3% of the  $\text{PM}_{2.5}$  in Zhengzhou (Geng *et al.*, 2103). This study focused on the major chemical components of  $\text{PM}_{2.5}$  and omitted the fine soil component, which was not included in the calculation. In this study, the factor used to convert OC to OM to account for the hydrogen, oxygen, and nitrogen present in the OM was changed from 1.4 to 1.6 (Turpin and Lim, 2001). Furthermore, the organic mass was divided into two fractions: POC (primary organic carbon) and SOC ( $[\text{OMC}] = 1.6\{[\text{POC}] + [\text{SOC}]\}$ ).

Fig. 6 provides the seasonal and annual extinction coefficients from 2011 to 2013. Generally, the annual mean extinction coefficients were 581, 566 and  $847 \text{ Mm}^{-1}$  for

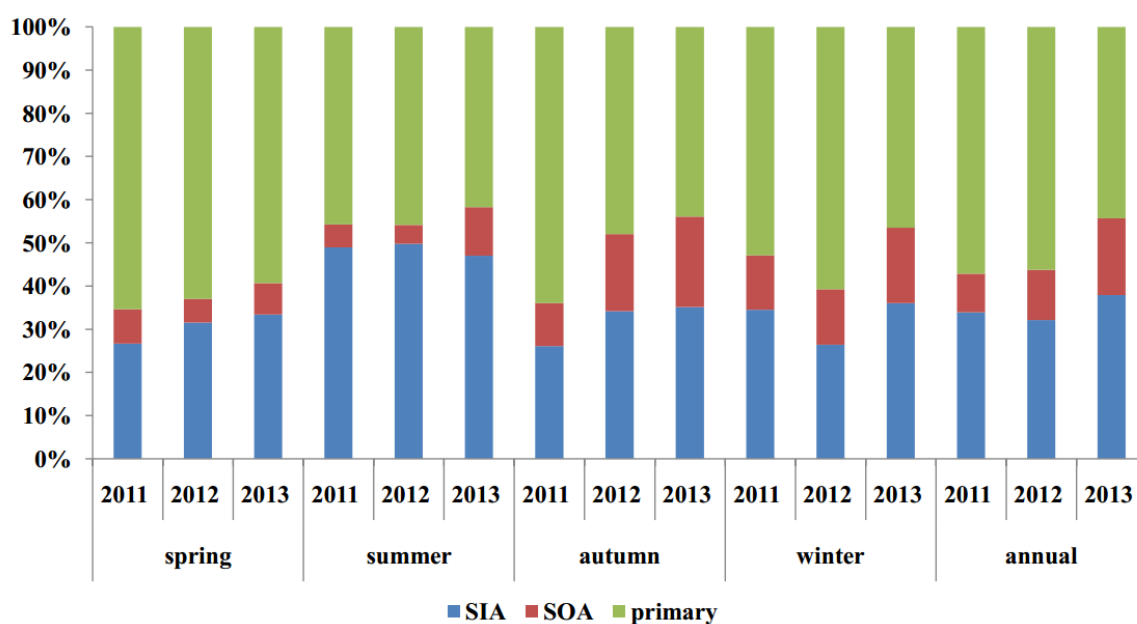


**Fig. 5.** Annual and seasonal contributions of the secondary components to the PM<sub>2.5</sub> mass concentrations during 2011–2013.

2011, 2012 and 2013, respectively, with the highest value (1212 Mm<sup>-1</sup>) occurring during the winter of 2013 and the lowest value (321 Mm<sup>-1</sup>) occurring during the summer of 2012. The concentrations of PM<sub>2.5</sub> and its individual components greatly increased from 2011 and 2012 to 2013, which caused the light extinction coefficient reconstructed by the components to increase by a greater amount in 2013. Higher values of the extinction coefficient indicate lower visibility. This result also reflects the important impacts of PM<sub>2.5</sub> on atmospheric visibility. In addition, the  $b_{ext}$  value at the Zhengzhou site was much higher than that obtained from the PM<sub>2.5</sub> reconstructed aerosol light extinction coefficient ( $b_{ext\_aer}$ ) in the IMPROVE regions over 2005–2008. These values were reported as 5.73 Mm<sup>-1</sup> in the Great Basin in January, 127.26 Mm<sup>-1</sup> in Appalachia, USA, in August (rural) and 246.09 Mm<sup>-1</sup> in urban Fresno CA, USA, in December (Hand *et al.*, 2011). Therefore, the visibility in the Zhengzhou region was very poor.

Fig. 7 shows the seasonal and annual percentages of the contributions of the chemical species to the light extinction coefficient. As shown in Fig. 7, (NH<sub>4</sub>)<sub>2</sub>SO<sub>4</sub> contributed the most (37–42%) to  $b_{ext}$  according to the annual average results, followed by NH<sub>4</sub>NO<sub>3</sub> (23–25%), SOM (11–19%), POM (9–13%) and EC (8–11%). The percentages of SOM increased by 8% from 2011 to 2013, while those of the other species decreased in 2013. The secondary aerosols ((NH<sub>4</sub>)<sub>2</sub>SO<sub>4</sub> + NH<sub>4</sub>NO<sub>3</sub> + SOM) accounted for 76–83% of the total  $b_{ext}$ , with sulfate and nitrate ((NH<sub>4</sub>)<sub>2</sub>SO<sub>4</sub> + NH<sub>4</sub>NO<sub>3</sub>) accounting for 61–67%. These results implied that sulfate was the largest contributor to visibility degradation. However, the secondary species, particularly SIA, played a dominant role in the degradation of visibility in Zhengzhou. The major species that influenced the visibility depended on the region. The light extinction contributions that were reported for the spring of 2007 in Guangzhou, China (Tao *et al.*, 2009), were as follows: (NH<sub>4</sub>)<sub>2</sub>SO<sub>4</sub> (40 ± 6%) > OM (22 ± 4%) ≈

EC (22 ± 4%) > NH<sub>4</sub>NO<sub>3</sub> (16 ± 4%). These contributions were different from those in Zhengzhou. The significant contributions of (NH<sub>4</sub>)<sub>2</sub>SO<sub>4</sub> + NH<sub>4</sub>NO<sub>3</sub> to the degradation of visibility resulted from the relatively high percentage of SIA in PM<sub>2.5</sub>.

In terms of seasonal percentages, (NH<sub>4</sub>)<sub>2</sub>SO<sub>4</sub> contributed the most to PM<sub>2.5</sub> during the summer. NH<sub>4</sub>NO<sub>3</sub> and SOM had the highest contributions during the autumn, and these species exhibited seasonal patterns that were similar to those of the mass-based contributions to PM<sub>2.5</sub>. Overall, secondary aerosols ((NH<sub>4</sub>)<sub>2</sub>SO<sub>4</sub> + NH<sub>4</sub>NO<sub>3</sub> + SOM) accounted for 80% of  $b_{ext}$ , and primary aerosols (POM + EC) accounted for 20%. Clearly, secondary aerosols played a dominant role in the degradation of visibility in Zhengzhou. The same conclusion has been reported for other cities in the Pearl River Delta in China (Deng *et al.*, 2013), where the extinction contribution of secondary aerosols was 60% in the dry environment ( $f(RH) \approx 1.0$ ) and increased to 75% and 82% at RH = 80% ( $f(RH) \approx 3.0$ ) and 95% ( $f(RH) \approx 6.0$ ), respectively. These values are closely related to the high  $f(RH)$  values that are used to calculate  $b_{ext}$  in the Pearl River Delta.

Even when considering all of the involved uncertainties (e.g., the variable RH, empirical equations and magnitudes of the coefficients), the secondary species still played an important role in PM<sub>2.5</sub>. NO<sub>x</sub> and VOCs emissions drive photochemical reactions and their associated oxidants. Secondary fine particles are formed from photochemical and other reactions that involve precursor gases, such as SO<sub>2</sub>, NO<sub>x</sub>, NH<sub>3</sub> and VOCs. Most cities lack routine VOC measurements, and control of NH<sub>3</sub> and VOCs is lacking. Therefore, reducing secondary species by strengthening the control of SIA and SOA precursors, such as NO<sub>x</sub>, SO<sub>2</sub>, NH<sub>3</sub> and VOCs, will play an important role in controlling China's PM<sub>2.5</sub> levels and reducing their influences on the environment.

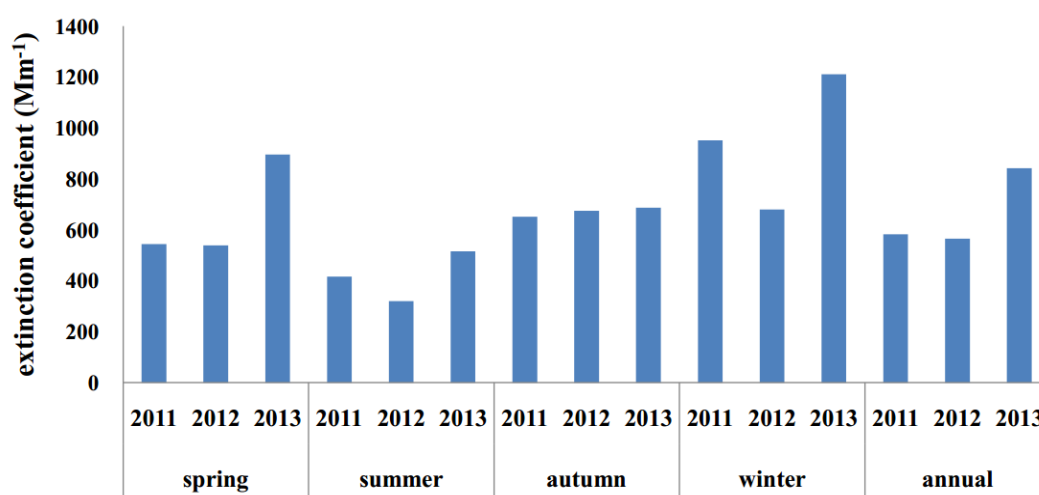


Fig. 6. Extinction coefficients from 2011 to 2013.

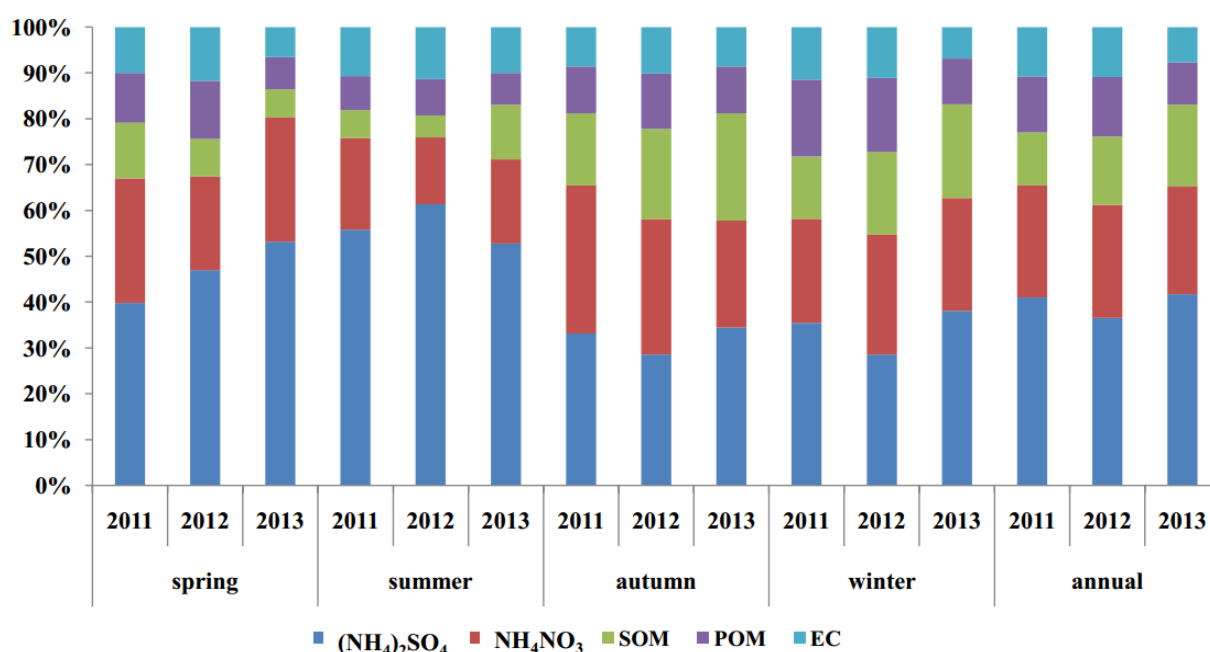


Fig. 7. Annual and seasonal extinction contributions of the individual components to PM<sub>2.5</sub>.

## SUMMARY AND CONCLUSIONS

The annual mean concentrations of PM<sub>2.5</sub> were 186, 180 and 218  $\mu\text{g m}^{-3}$  in 2011, 2012 and 2013, respectively. The PM<sub>2.5</sub> levels in Zhengzhou were 5–6 times greater than the values listed by the National Ambient Air Quality Standard of China (annual value of 35  $\mu\text{g m}^{-3}$ ). Thus, severe PM<sub>2.5</sub> pollution occurs in Zhengzhou. The general increases observed in PM<sub>2.5</sub>, particularly in SIA and SOC, are associated with increases in the number of vehicles and the total energy consumption in Zhengzhou. Regulatory agencies should strictly enforce air pollution control measures and identify effective measures for reducing primary and secondary PM<sub>2.5</sub> to control air pollution.

Regarding the annual average PM<sub>2.5</sub>, OM was the largest contributor (18–26%), followed by SO<sub>4</sub><sup>2-</sup> (14–19%), NO<sub>3</sub><sup>-</sup>

(10–11%), NH<sub>4</sub><sup>+</sup> (8–9%) and EC (3%). From 2011 to 2013, the contribution of OM increased by 8%, and that of SO<sub>4</sub><sup>2-</sup> increased by 3%. The relatively stable EC concentration revealed improvements in combustion technologies despite the increasing energy consumption. Moreover, measures should be taken to reduce the increasing OC concentration and prevent the exacerbation of OM pollution.

As indicated by the NO<sub>3</sub><sup>-</sup>/SO<sub>4</sub><sup>2-</sup> mass ratio, stationary source emissions remain an important contributor of fine particles in Zhengzhou. Obvious SOC enrichment can be observed during the winter and autumn, most likely due to biomass burning and increased coal combustion during the autumn and winter.

An investigation of secondary species revealed that secondary aerosols played a dominant role in the total mass of PM<sub>2.5</sub> and the degradation of visibility. SIA accounted

for 26–50% of the PM<sub>2.5</sub> mass, while SOM accounted for 4–21%. In addition, secondary aerosols ((NH<sub>4</sub>)<sub>2</sub>SO<sub>4</sub> + NH<sub>4</sub>NO<sub>3</sub> + SOC) accounted for 80% of the *b<sub>ext</sub>*, and (NH<sub>4</sub>)<sub>2</sub>SO<sub>4</sub> and NH<sub>4</sub>NO<sub>3</sub> were the main factors related to poor visibility in Zhengzhou.

To achieve PM<sub>2.5</sub> pollution control targets, measures must be taken to control NO<sub>x</sub>, SO<sub>2</sub>, NH<sub>3</sub> and VOC emissions.

## ACKNOWLEDGMENTS

This study was supported by the Ministry of Environmental Protection of the People's Republic of China (grant no. 201409010). The authors would like to thank those who assisted with the analyses: Yuanqian Xu, Junhua Wei, Yinan Gao, and Panru Kang.

## REFERENCES

- Alves, C.A., Pio, C.A. and Duarte, A.C. (2000). Particle Size Distributed Organic Compounds in a Forest Atmosphere. *Environ. Sci. Technol.* 25: 2133–2140.
- Anderson, J.O., Thundiyil, J.G. and Stolbach, A. (2012). Clearing the Air: A Review of the Effects of Particulate Matter Air Pollution on Human Health. *J. Med. Toxicol.* 8: 166–175.
- Behra, S.N. and Sharma, M. (2010). Reconstructing Primary and Secondary Components of PM<sub>2.5</sub> Composition for an Urban Atmosphere. *Aerosol Sci. Technol.* 44: 983–992.
- Cabada, J.C., Pandis, S.N. and Robinson, A.L. (2002). Sources of Atmospheric Carbonaceous Particulate Matter in Pittsburgh, Pennsylvania. *J. Air Waste Manage. Assoc.* 52: 732–741.
- Cabada, J.C., Pandis, S.N., Subramanian, R., Robinson, A.L., Polidori, A. and Turpin, B. (2004). Estimating the Secondary Organic Aerosol Contribution to PM<sub>2.5</sub> Using the EC Tracer Method. *Aerosol Sci. Technol.* 38: 140–155.
- Cao, J., Lee, S.C., Chow, J.C., Watson, J.G., Ho, K.F., Zhang, R., Jin, Z., Shen, Z., Chen, G., Kang, Y., Zou, S., Zhang, L., Qi, S., Dai, M., Cheng, Y. and Hu, K. (2007). Spatial and Seasonal Distributions of Carbonaceous Aerosols over China. *J. Geophys. Res.* 112: D22S11, doi: 10.1029/2006JD008205.
- Castro, L.M., Pio, C.A., Harrison, R.M. and Smith, D.J.T. (1999). Carbonaceous Aerosol Particles in Urban and Rural European Atmospheres: Estimation of Secondary Organic Carbon Concentrations. *Atmos. Environ.* 33: 2771–2281.
- Chen, Y., Zhi, G., Feng, Y., Fu, J., Feng, J., Sheng, G. and Simoneit, B.R.T. (2006). Measurements of Emission Factors for Primary Carbonaceous Particles from Residential Raw-Coal Combustion in China. *Geophys. Res. Lett.* 33: L20815, doi: 10.1029/2006GL026966.
- Chow, J.C., Watson, J.G., Crow, D., Lowenthal, D.H. and Merrifield, T. (2001). Comparison of IMPROVE and NIOSH Carbon Measurement. *Aerosol Sci. Technol.* 34: 23–34.
- Chung, S.H. and Seinfeld, J.H. (2002). Global Distribution and Climate Forcing of Carbonaceous Aerosols. *J. Geophys. Res.* 107: AAC 14–1–AAC 14–33, doi: 10.1029/2001JD001397.
- CSC (Chinese State Council) (2013). Atmospheric Pollution Prevention and Control Action Plan, [http://www.gov.cn/zwggk/2013-09/12/content\\_2486773.htm](http://www.gov.cn/zwggk/2013-09/12/content_2486773.htm) (in Chinese).
- Deng, X., Wu, D., Yu, J., Lau, A.K., Li, F., Tan, H., Yuan, Z., Ng, W.M., Deng, T., Wu, C. and Zhou, X. (2013). Characterization of Secondary Aerosol and Its Extinction Effects on Visibility over the Pearl River Delta Region, China. *J. Air Waste Manage. Assoc.* 63: 1012–1021.
- DEPH (Department of Environmental Protection of Henan Province) (2013). <http://www.hnep.gov.cn/tabid/435/InfOID/7068/Default.aspx>(in Chinese), Published : June 4 2013.
- DEPH (Department of Environmental Protection of Henan Province) (2014). <http://www.hnep.gov.cn/tabid/435/InfOID/11750/Default.aspx> (in Chinese), Published : June 3 2014.
- Duarte, R.M.B.O., Mieiro, C.L., Penetra, A., Pio, C.A. and Duarte, A.C. (2008). Carbonaceous Materials in Size-Segregated Atmospheric Aerosols from Urban and Coastal-Rural Areas at the Western European Coast. *Atmos. Res.* 90: 253–263.
- EMSC (Environment Monitoring Station of China) (2013). The Air Quality Status Report of 74 Cities in January 2013, [http://www.cnemc.cn/publish/totalWebSite/news/news\\_33891.html](http://www.cnemc.cn/publish/totalWebSite/news/news_33891.html) (in Chinese), Published: February 7 2013.
- Fan, C., Wang, X., Wang, Y., Liu, F. and Wu, C. (2012). Anthropogenic Total Emissions and Distribution of Non-methane Volatile Organic Compounds in China. *Sichuan Environment.* 31: 82–87 (in Chinese).
- Gao, X., Yang, L., Cheng, S., Gao, R., Zhou, Y., Xue, L., Shou, Y., Wang, J., Wang, X., Nie, W., Xu, P. and Wang, W. (2011). Semi-Continuous Measurement of Water-Soluble Ions in PM<sub>2.5</sub> in Jinan, China: Temporal Variations and Source Apportionments. *Atmos. Environ.* 45: 6048–6056.
- Geng, N., Wang, J., Xu, Y., Zhang, W., Chen, C. and Zhang, R. (2013). PM<sub>2.5</sub> in an Industrial District of Zhengzhou, China: Chemical Composition and Source Apportionment. *Particuology* 11: 99–109.
- Hand, J.L., Copeland, S.A., Day, D.E., Dillner, A.M., Indresand, H., Malm, W.C., McDade, C.E., Moore, C.T., Pitchford, M.L., Schichtel, B.A. and Watson, J.G. (2011). Spatial and Seasonal Patterns and Temporal Variability of Haze and Its Constituents in the United States, Report V. IMPROVE Reports, [http://vista.cira.colostate.edu/improve/Publications/improve\\_reports.htm](http://vista.cira.colostate.edu/improve/Publications/improve_reports.htm).
- Henan Statistical Yearbook 2011 (2012). China Statistics Press, Beijing.
- Henan Statistical Yearbook 2012 (2013). China Statistics Press, Beijing.
- Henan Statistical Yearbook 2013 (2014). China Statistics Press, Beijing.
- Hu, G., Sun, J., Zhang, Y., Shen, X. and Yang, Y. (2015). Chemical Composition of PM<sub>2.5</sub> Based on Two-Year Measurements at an Urban Site in Beijing. *Aerosol Air Qual. Res.* 15: 1748–1759, doi: 10.4209/aaqr.2014.11.0284.

- IMPROVE (Interagency Monitoring of Protected Visual Environments) (b). Relative Humidity Adjustment Factors,  $f(\text{RH})$ , [http://vista.cira.colostate.edu/improve/Tools/humidity\\_correction.htm](http://vista.cira.colostate.edu/improve/Tools/humidity_correction.htm).
- IMPROVE (Interagency Monitoring of Protected Visual Environments) (a). Reconstructing Light Extinction from Aerosol Measurements, <http://vista.cira.colostate.edu/improve/Tools/ReconBext/reconBext.htm>.
- Kim, B.M., Teffera, S. and Zeldin, M.D. (2000). Characterization of  $\text{PM}_{2.5}$  and  $\text{PM}_{10}$  in the South Coast Air Basin of Southern California: Part I Spatial Variations. *J. Air Waste Manage. Assoc.* 50: 2034–2044.
- Kim, Y.J., Kim, K.W., Kim, S.D., Lee, B.K. and Han, J.S. (2006). Fine Particulate Matter Characteristics and Its Impact on Visibility Impairment at Two Urban Sites in Korea: Seoul and Incheon. *Atmos. Environ.* 40: 593–605.
- Koch, D., Bond, T.C., Streets, D., Unger, N. and van der Werf, G.R. (2007). Global Impacts of Aerosols from Particular Source Regions and Sectors. *J. Geophys. Res.* 112, doi: 10.1029/2005JD007024.
- Liousse, C., Penner, J.E., Chuang, E.C., Walton, J.J., Eddleman, H. and Cachier, H. (1996). A Global Three-Dimensional Model Study of Carbonaceous Aerosols. *J. Geophys. Res.* 101: 19411–19432.
- McCulloch, A., Aucott, M.L., Benkovitz, C.M., Graedel, T.E., Kleiman, G., Midgley, P.M. and Li, Y.F. (1999). Global Emissions of Hydrogen Chloride and Chloromethane from Coal Combustion, Incineration and Industrial Activities: Reactive Chlorine Emissions Inventory. *J. Geophys. Res.* 104: 8391–8403.
- Niu, Z., Zhang, F., Kong, X., Chen, J., Yin, L. and Xu, L. (2012). One-Year Measurement of Organic and Elemental Carbon in Size-Segregated Atmospheric Aerosol at a Coastal and Suburban Site in Southeast China. *J. Environ. Monit.* 14: 2961–2967.
- Schaap, M., Spindler, G., Schultz, M., Acker, K., Maenhaut, W., Berner, A., Wiedprecht, W., Streit, N., Müller, K., Brüggeman, E., Chi, X., Putaud, J.P., Hitzinger, R., Puxbaum, H., Baltensperger, U. and ten Brink, H. (2004). Artefacts in the Sampling of Nitrate Studied in the “INTERCOMP” Campaigns of EUROTRACAEROSOL. *Atmos. Environ.* 38: 6487–6496.
- Schauer, J.J., Kleeman, M.J., Cass, G.R. and Simoneit, B.R.T. (1999). Measurement of Emissions from Air Pollution Sources. 2.  $\text{C}_1$  through  $\text{C}_{30}$  Organic Compounds from Medium Duty Diesel Trucks. *Environ. Sci. Technol.* 33: 1578–1587.
- Schauer, J.J., Kleeman, M.J., Cass, G.R. and Simoneit, B.R.T. (2002). Measurement of Emissions from Air Pollution Sources. 5.  $\text{C}_1$ - $\text{C}_{32}$  Organic Compounds from Gasoline-Powered Motor Vehicles. *Environ. Sci. Technol.* 36: 1169–1180.
- Shi, H., Qi, Y. and Liu, Y. (2010). Research of Environmental Effects about Rural Energy Consumption. *China Popul. Resour. Environ.* 20: 148–153.
- Squizzato, S., Masiol, M., Brunelli, A., Pistollato, S., Tarabotti, E., Rampazzo, G. and Pavoni, B. (2013). Factors Determining the Formation of Secondary Inorganic Aerosol: A Case Study in the Po Valley (Italy). *Atmos. Chem. Phys.* 13: 1927–1939.
- Tao, J., Ho, K., Chen, L., Zhu, L., Han, J. and Xu, Z. (2009). Effect of Chemical Composition of  $\text{PM}_{2.5}$  on Visibility in Guangzhou, China, 2007 Spring. *Particuology* 7: 68–75.
- Turpin, B.J. and Lim, H.J. (2001). Species Contributions to  $\text{PM}_{2.5}$  Mass Concentrations: Revisiting Common Assumptions for Estimating Organic Mass. *Aerosol Sci. Technol.* 35: 602–610.
- US EPA (US Environmental Protection Agency) (1999). *Visibility Monitoring Guidance Document*. EPA-454/R-99-003, U.S. Environmental Protection Agency, Washington, DC.
- Valavanidis, A., Fiotakis, K. and Vlachogianni, T. (2008). Airborne Particulate Matter and Human Health: Toxicological Assessment and Importance of Size and Composition of Particles for Oxidative Damage and Carcinogenic Mechanisms. *J. Environ. Sci. Health., Part C Environ. Carcinog. Ecotoxicol. Rev.* 26: 339–362.
- Vecchi, R., Valli, G., Fermo, P., D’Alessandro, A., Piazzalunga, A. and Bernardoni, V. (2009). Organic and Inorganic Sampling Artefacts Assessment. *Atmos. Environ.* 43: 1713–1720.
- Voutsas, D., Samara, C., Manoli, E., Lazarou, D. and Tzoumaka, P. (2014). Ionic Composition of  $\text{PM}_{2.5}$  at Urban Sites of Northern Greece: Secondary Inorganic Aerosol Formation. *Environ. Sci. Pollut. Res.* 21: 4995–5006.
- Wang, H., Hao, Z., Zhuang, Y., Wang, W. and Liu, X. (2008). Characterization of Inorganic Components of Size-Segregated Particles in the Flue Gas of a Coal-Fired Power Plant. *Energy Fuels* 22: 1636–1640.
- Wang, Y., Zhuang, G., Tang, A., Yuan, H., Sun, Y., Chen, S. and Zheng, A. (2005). The Ion Chemistry and the Source of  $\text{PM}_{2.5}$  Aerosol in Beijing. *Atmos. Environ.* 39: 3771–3784.
- Wang, Y., Zhuang, G., Zhang, X., Huang, K., Xu, C., Tang, A., Chen, J. and An, Z. (2006). The Ion Chemistry, Seasonal Cycle and Sources of  $\text{PM}_{2.5}$  and TSP Aerosol in Shanghai. *Atmos. Environ.* 40: 2935–2952.
- Warren, B., Austin, R.L. and Cocker, III, D.R. (2009). Temperature Dependence of Secondary Organic Aerosol. *Atmos. Environ.* 43:3548–3555.
- Wittmaack, K. and Keck, L. (2004). Thermodesorption of Aerosol Matter on Multiple Filters of Different materials for a More Detailed Evaluation of Sampling Artifacts. *Atmos. Environ.* 38: 5205–5215.
- Xu, W., Chen, H., Li, D., Zhao, F. and Yang, Y. (2013). A Case Study of Aerosol Characteristics during a Haze Episode over Beijing. *Procedia Environ. Sci.* 18: 404–411.
- Yao, X., Chan, C.K., Fang, M., Cadle, S., Chan, T., Mulawa, P., He, K. and Ye, B. (2002). The Water-Soluble Ionic Composition of  $\text{PM}_{2.5}$  in Shanghai and Beijing, China. *Atmos. Environ.* 36: 4223–4234.
- Zdziennicka, A., Szymczyk, K. and Janczuk, B. (2009). Correlation between Surface Free Energy of Quartz and Its Wettability by Aqueous Solutions of Nonionic, Anionic and Cationic Surfactants. *J. Colloid Interface Sci.* 340: 243–248.
- Zhang, Y., Shao, M., Zhang, Y., Zeng, L., He, L., Zhu, B.,

- Wei, Y. and Zhu, X. (2007). Source Profiles of Particulate Organic Matters Emitted from Cereal Straw Burnings. *J. Environ. Sci.* 19: 167–175.
- Zhou, C. (2013). Study on Energy Consumption Structure of Zhengzhou. *Mark Res.* 3: 54–57 (in Chinese).
- Zhao, M. (2014). An Empirical Analysis of the Relationship between Our Country Tax Revenue Growth and GDP Growth. *Technological Development of Enterprise* 33: 118–120 (in Chinese).

*Received for review, January 4, 2015*

*Revised, April 9, 2015*

*Accepted, July 31, 2015*